

## Chapter 3

# Magnets

### 3.1 Overview

The Large Hadron Collider relies on superconducting magnets that are at the edge of present technology. Other large superconducting accelerators (Tevatron-FNAL, HERA-DESY and RHIC-BNL) all use classical NbTi superconductors, cooled by supercritical helium at temperatures slightly above 4.2 K, with fields below or around 5 T. The LHC magnet system, while still making use of the well-proven technology based on NbTi Rutherford cables, cools the magnets to a temperature below 2 K, using superfluid helium, and operates at fields above 8 T. One detrimental effect of reducing the temperature by more than a factor of two is the reduction of the heat capacity of the cable by almost an order of magnitude. As a result, for a given temperature margin (difference between the critical temperature of the superconductor and the operating temperature), the energy deposition that can trigger a quench is substantially reduced. This means that the temperature margin must be significantly larger than that used in previous projects and that a tighter control of movements and heat dissipation inside cables is needed. Since the electromagnetic forces increase with the square of the field, the structures retaining the conductor motion must be mechanically much stronger than in earlier designs.

In addition, space limitations in the tunnel and the need to keep costs down have led to the adoption of the “two-in-one” or “twin-bore” design for almost all of the LHC superconducting magnets. The two-in-one design accommodates the windings for the two beam channels in a common cold mass and cryostat, with magnetic flux circulating in the opposite sense through the two channels. This makes the magnet structure complicated, especially for the dipoles, for which the separation of the two beam channels is small enough that they are coupled both magnetically and mechanically.

### 3.2 Superconducting cable

The transverse cross-section of the coils in the LHC 56 mm aperture dipole magnet (figure 3.1) shows two layers of different cables distributed in six blocks. The cable used in the inner layer has 28 strands, each having a diameter of 1.065 mm, while the cable in the outer layer is formed

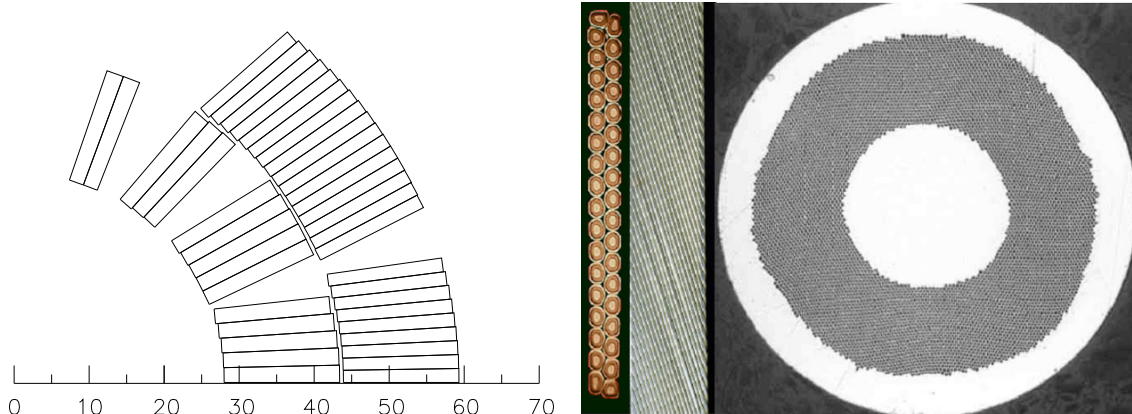


**Figure 3.1:** Conductor distribution in the dipole coil cross-section ( $X$ -axis in mm on left). Picture of cables and strand on right.

from 36 strands, each of 0.825 mm diameter. The main parameters of the two cables are given in table 3.1.

The filament size chosen ( $7\ \mu\text{m}$  for the strand of the inner layer cable and  $6\ \mu\text{m}$  for the strand of the outer layer cable) allows the fabrication of superconducting wires by a single stacking process. The filament size for each type of strand is optimised in order to reduce the effects of the persistent currents on the sextupole field component at injection. The residual errors are corrected by small sextupole and decapole magnets located at the end of each dipole.

Table 3.2 shows the peak field ( $B_p$ ) for the two layers of cable, the field margin and the temperature margin when the magnet operates at 8.33 T. The field margin is defined as the ratio of the operating field to the expected quenching field at the short-sample limit ( $B_{ss}$ ). The reference temperature of the bath is 1.9 K (helium between coil inner radius and cold bore). Also shown are the current density in the copper at  $B_0 = 8.33\ \text{T}$ , and, in the case of a quench, the expected hot-spot temperature in the outer layer and maximum quench voltage, calculated in the adiabatic approximation.

During ramping and discharge of the current in the dipole magnet, the main losses and field errors are generated by inter-strand coupling currents and by persistent currents inside the filaments. The power losses due to inter-strand coupling currents depend strongly on the coating of the strands and the compression of the coils at low temperature. They are proportional to  $(dB/dt)^2$  and inversely proportional to the inter-strand contact resistance  $R_c$ . Losses for a twin-aperture dipole have been estimated at 180 mW/m for a charging time of 1200 s, corresponding to an energy of 220 J/m transmitted to the helium bath and to specific power dissipation in the cables of  $0.077\ \text{mW/cm}^3$ .

In the case of a discharge of the machine, the upper limit of the time constant is given by the characteristics of the diode heat sink of the quench protection system and the quench propagation to other magnets via bus-bars. In the 10 m long magnets tested, a linear discharge from 8.33 T with  $dB/dt$  of 0.12 T/s did not initiate a quench. An exponential discharge with a time constant of 100 s leads to a load of 500 J/m. These values are mainly due to hysteresis losses and are calculated with an inter-strand contact resistance of  $10\ \mu\Omega$ , the lowest expected.

**Table 3.1:** Strand and cable characteristics of main dipoles (MB) and main quadrupoles (MQ).

	Inner Layer MB	Outer Layer MB Both layers MQ
<b>Strand</b>		
Coating type	Sn5wt%Ag	Sn5wt%Ag
Diameter after coating [mm]	$1.065 \pm 0.0025$	$0.825 \pm 0.0025$
Copper to superconductor ratio	$1.65 \pm 0.05$	$1.95 \pm 0.05$
Filament diameter [ $\mu\text{m}$ ]	7	6
Number of filaments	$\sim 8'900$	$\sim 6'500$
RRR	$\geq 150$	$\geq 150$
Twist pitch after cabling [mm]	$18 \pm 1.5$	$15 \pm 1.5$
Critical current [A] 10 T, 1.9 K	$\geq 515$	$\geq 380$
9 T, 1.9 K		$\geq 380$
$\Delta M$ AT 0.5 T AND 1.9 K [MT]	$\leq 30$	$\leq 23$
<b>Cable</b>		
Number of strands	28	36
Cable dimension (at room temperature)		
Mid-thickness at 50 MPa [mm]	$1.900 \pm 0.006$	$1.480 \pm 0.006$
Thin edge [mm]	1.736	1.362
Thick edge [mm]	2.064	1.598
Width [mm]	$15.10_{+0}^{-0.02}$	$15.10_{+0}^{-0.02}$
Keystone angle [degree]	$1.25 \pm 0.05$	$0.90 \pm 0.05$
Transposition pitch [mm]	$115 \pm 5$	$100 \pm 5$
Aspect ratio	7.95	10.20
MIITS [300 K] [ $\text{MA}^2 \text{s}$ ]	45 [8T]	30 [6T]
Critical current $I_c$ [A] 10 T, 1.9 K	$> 13750$	$> 12960$
9 T, 1.9 K		$> 12960$
$dI_c/dB$ [A/T]	$> 4800$	$> 3650$
Inter-strand cross contact resistance [ $\mu\Omega$ ]	$\geq 15$	$\geq 40$
RRR	$\geq 70$	$\geq 70$
No cold welds and no cross-overs of strands allowed		

**Table 3.2:** Expected quench performance and temperature margin ( $B_0 = 8.33 \text{ T}$ ,  $I_0 = 11'800 \text{ A}$ ,  $T_{\text{bath}} = 1.9 \text{ K}$ ).

Layer	$B_p$ [T]	$B_{\text{margin}}$ [%]	$\Delta T$ [K] margin	$J_{\text{cu}}$ [A/mm <sup>2</sup> ]	$T_{\text{max quench}}$ [K]	$V_{\text{max}}$ [V]
Inner layer	8.57	85.7	1.51	760		
Outer Layer	7.46	85.8	1.57	928	375	500

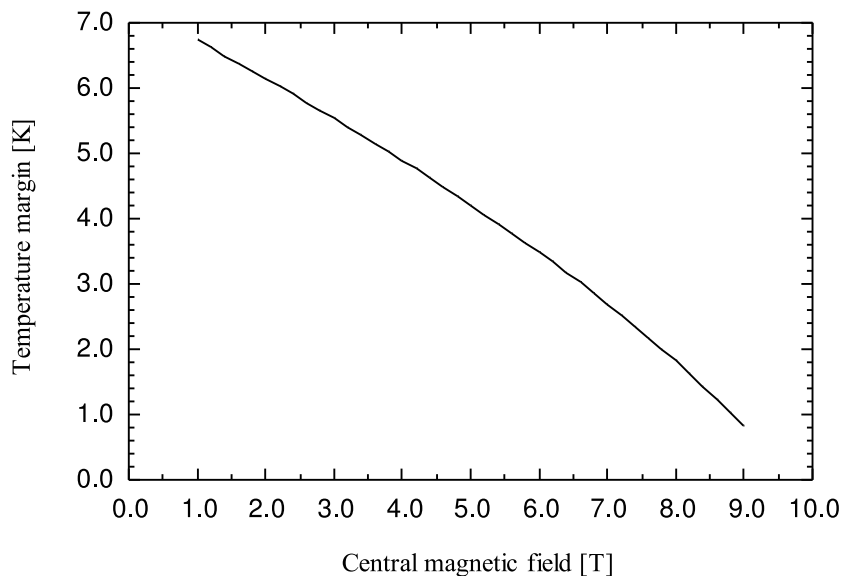


**Figure 3.2:** Variation of the temperature margin of the inner layer for  $T_{\text{bath}} = 1.9$  K.

A superconductor stays in the superconducting state when the temperature, the magnetic field, and the current density are below their critical values. The temperature margin shown in table 3.2 corresponds to the difference between the bath temperature and the critical temperature at the design field and current. The temperature margin as a function of the operating field for the inner layers, and for a bath temperature of 1.9 K, is shown in figure 3.2.

### 3.3 Main dipole cold mass

The LHC ring accommodates 1'232 main dipoles: 1'104 in the arc and 128 in the DS regions. They all have the same basic design. The geometric and interconnection characteristics have been targeted to be suitable for the DS region, which is more demanding than the arc. The cryodipoles are a critical part of the machine, both from the machine performance point of view and in terms of cost. Figure 3.3 shows the cross section of the cryodipole. The three European companies that have been collaborating with CERN throughout the prototype phase manufactured the series cryodipole cold masses. To reduce costs, co-ordinate orders, and obtain the highest possible degree of uniformity, CERN supplies most of the critical components and some of the main tooling. Thus CERN becomes, all at the same time: the magnet designer, the supplier of superconducting cables and most components, and the client. The dipole manufacturers are responsible for good quality construction that is free from faults. In order to help the cold mass manufacturers during the start-up phase, there have been two contracts with each manufacturer: first a pre-series contract (for the first 30 cold masses), then a series contract (for the remaining 386 cold masses). The components supplied by CERN for the two types of contract are shown in table 3.3.

Tests on the first 15 m-long prototype of the second generation showed that transport of the fully assembled cryodipole is critical. For this reason, the cold masses are put in their cryostats at CERN. Apart from the obvious cryogenics and vacuum considerations, the cryostating is also

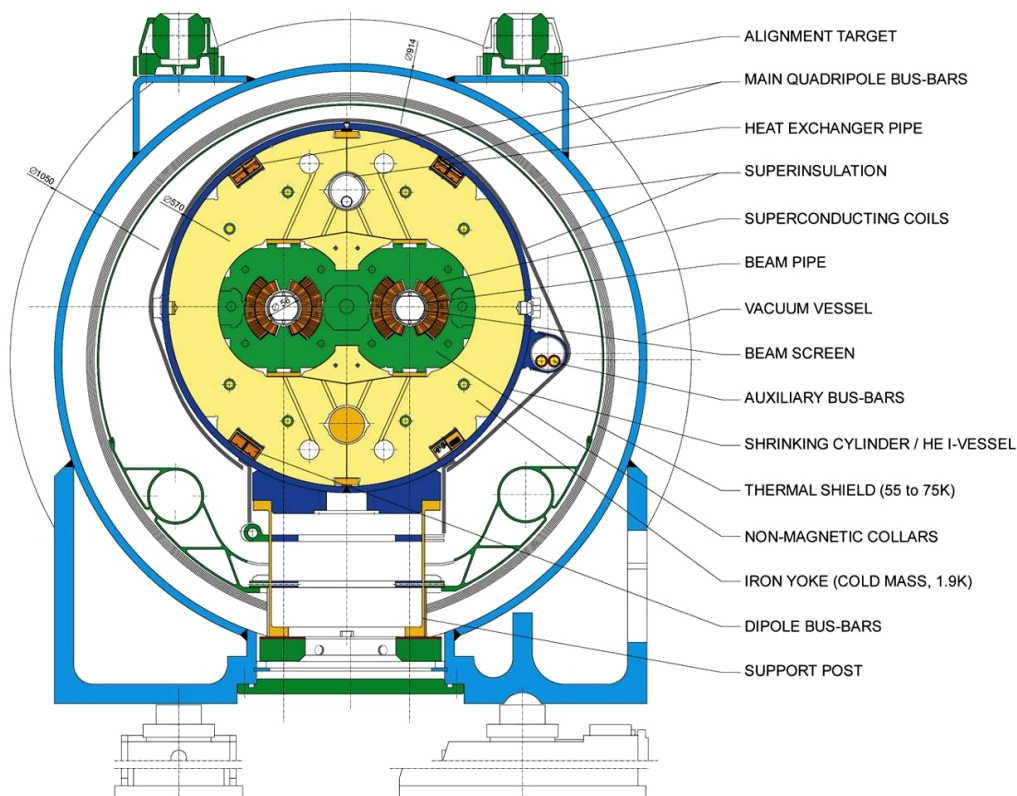


**Figure 3.3:** Cross-section of cryodipole (lengths in mm).

an important operation for the geometry and the alignment of the magnet, which is critical for the performance of the magnets in view of the large beam energy and small bore of the beam pipe. The core of the cryodipole is the “dipole cold mass”, which contains all the components cooled by superfluid helium. Referring to figure 3.3, the dipole cold mass is the part inside the shrinking cylinder/He II vessel. The dipole cold mass provides two apertures for the cold bore tubes (i.e. the tubes where the proton beams will circulate) and is operated at 1.9 K in superfluid helium. It has an overall length of about 16.5 m (ancillaries included), a diameter of 570 mm (at room temperature), and a mass of about 27.5 t. The cold mass is curved in the horizontal plane with an apical angle of 5.1 mrad, corresponding to a radius of curvature of about 2’812 m at 293 K, so as to closely match the trajectory of the particles. The main parameters of the dipole magnets are given in table 3.4.

The successful operation of LHC requires that the main dipole magnets have practically identical characteristics. The relative variations of the integrated field and the field shape imperfections must not exceed  $\sim 10^{-4}$ , and their reproducibility must be better than  $10^{-4}$  after magnet testing and during magnet operation. The reproducibility of the integrated field strength requires close control of coil diameter and length, of the stacking factor of the laminated magnetic yokes, and possibly fine-tuning of the length ratio between the magnetic and non-magnetic parts of the yoke. The structural stability of the cold mass assembly is achieved by using very rigid collars, and by opposing the electromagnetic forces acting at the interfaces between the collared coils and the magnetic yoke with the forces set up by the shrinking cylinder. A pre-stress between coils and retaining structure

**Table 3.3:** CERN supplied components for the dipole cold masses.

<b>Component</b>	<b>“Pre-Series” Contract</b>	<b>“Series” Contract</b>
Superconducting cables (for inner & outer layers)	x	x
Polyimide tapes for cable and Cu wedges, insulation (two types)	x	x
Copper wedges (4 types)	x	x
Head spacers sets (for inner & outer layers)	x	
Inter-layer spacers	x	
Layer-jump boxes	x	
Layer-jump filling pieces	x	
Cable stabilisers (3 types)	x	
Quench heaters	x	
Polyimide (in rolls) for the coils’ ground insulation	x	x
Collars (6 types)	x	x
Cold Bore tubes (insulated)	x	x
Low-carbon steel half-yoke & insert laminations	x	x
Non-magnetic steel half-yoke & insert laminations	x	x
Busbars subassemblies (ready to be mounted)	x	x
Shrinking half-cylinders	x	x
Spool piece correction magnets (sextupole and decapole/octupole)	x	x
End covers	x	x
Helium heat exchanger tube	x	x
Interconnection bellows	x	x
Instrumentation (including the wires) for the Cold Mass	x	x
Auxiliary busbar pipe	x	x

(collars, iron lamination and shrinking cylinder) is also built-in. Because of the larger thermal contraction coefficient of the shrinking cylinder and austenitic steel collars with respect to the yoke steel, the force distribution inside the cold mass changes during cool down from room temperature to 1.9 K. The sensitivity of the force distribution in the cold mass structure to the tolerances on all the major components and parameters (collars, laminations, inserts, coil pre-stress, and shrinking cylinder circumferential stress) has been checked by finite element analysis computations applying statistical methods. Some 3000 geometries were computed under high-field conditions; in all cases, strictly positive contact forces were found at the interfaces between yoke halves and between the yoke and collared coils.

The coils were manufactured in a clean area with adequate air circulation, air filtration, and an airlock access. Coil winding is done with a “winding machine”: see figure 3.4. During winding, the conductors and spacers are maintained in place by tools designed for this purpose. In particular, the conductor must always be clamped in place in the straight parts before winding the coil ends. Special tooling for forming and pressing the conductors at the ends is also used. After winding, the coil is prepared for the curing phase while still lying on the mandrels. This operation takes place in a dedicated curing press. This press is equipped with moulds whose inner diameter is the outer

**Table 3.4:** Main parameters of the dipole cold mass.

	<b>Value</b>	<b>Unit</b>
Injection field (0.45 TeV beam energy)	0.54	T
Current at injection field	763	A
Nominal field (7 TeV beam energy)	8.33	T
Current at nominal field	11850	A
Inductance at nominal field	98.7	mH
Stored energy (both apertures) at nominal field	6.93	MJ
Ultimate field	9.00	T
Current at ultimate field	12840	A
Stored energy (both apertures) at ultimate field	8.11	MJ
Maximum quench limit of the cold mass (from short samples)	9.7	T
Operating temperature	1.9	K
Magnetic length at 1.9 K and at nominal field	14312	mm
Distance between aperture axes at 1.9 K	194.00	mm
Cold mass sagitta at 293 K	9.14	mm
Bending radius at 1.9 K	2803.98	m
Inner coil diameter at 293 K	56.00	mm
Number of conductor blocks / pole	6	
Number of turns / pole, inner layer	15	
Number of turns / pole, outer layer	25	
Electromagnetic forces / coil quadrant at nominal field		
Horizontal force component (inner and outer layer)	1.8	MN/m
Vertical force component (inner and outer layer)	0.81	MN/m
Electromagnetic forces / coil quadrant at ultimate field		
Horizontal force component (inner and outer layer)	2.1	MN/m
Vertical force component (inner and outer layer)	0.94	MN/m
Axial electromagnetic force at each ends at nominal field	0.40	MN
Coil aperture at 293 K	56.00	mm
Cold tube inner diameter at 293 K	50.00	mm
Cold tube outer diameter at 293 K	53.00	mm
Cold mass length at 293 K (active part)	15.18	m
Cold mass diameter at 293 K	570.0	mm
Cold mass overall length with ancillaries	16.5	m
Total mass	~ 27.5	t

diameter of either the inner or the outer layer. In addition, the moulds are equipped with heating systems that allow the coils to be cured at  $190\pm 3^\circ\text{C}$  under a maximum pressure of 80-90 MPa.

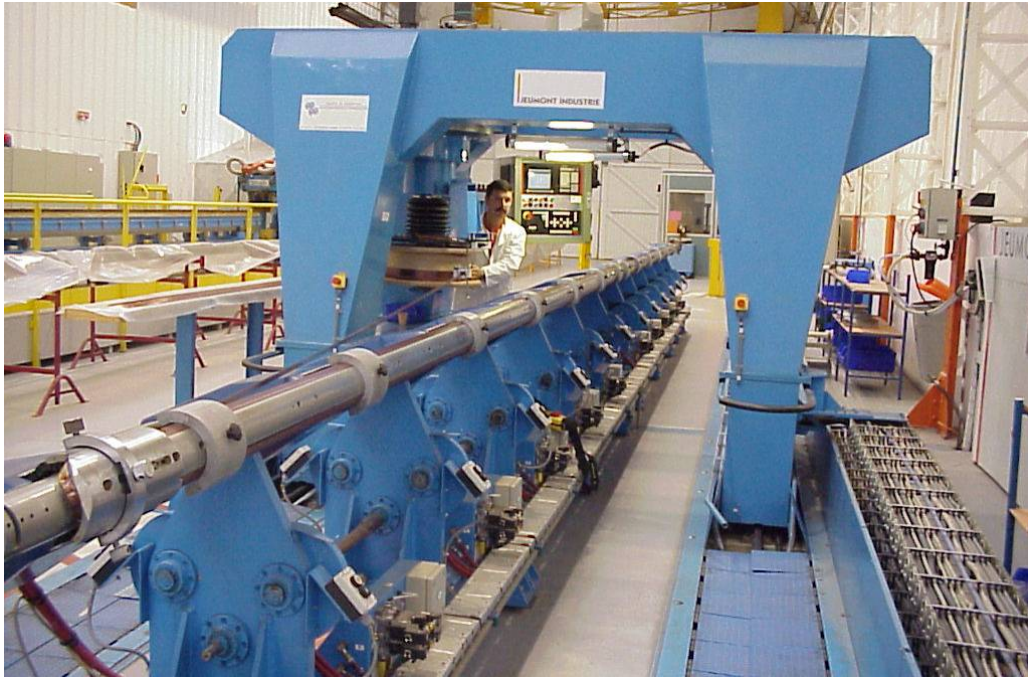


**Figure 3.4:** A winding machine for the superconducting coils.

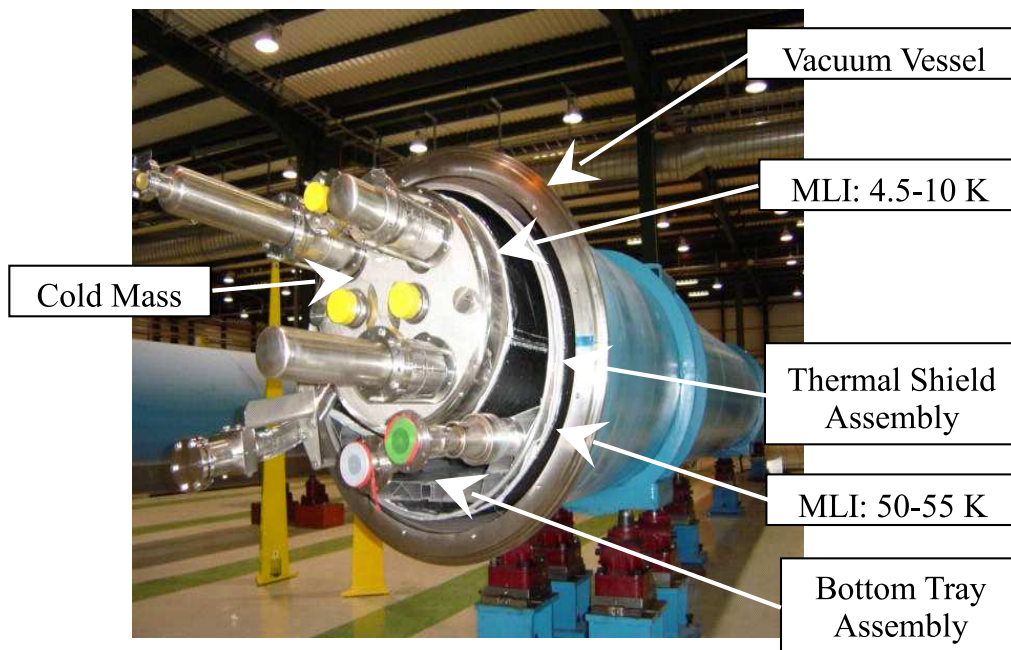


**Figure 3.5:** LHC dipole cryomagnet assembly.

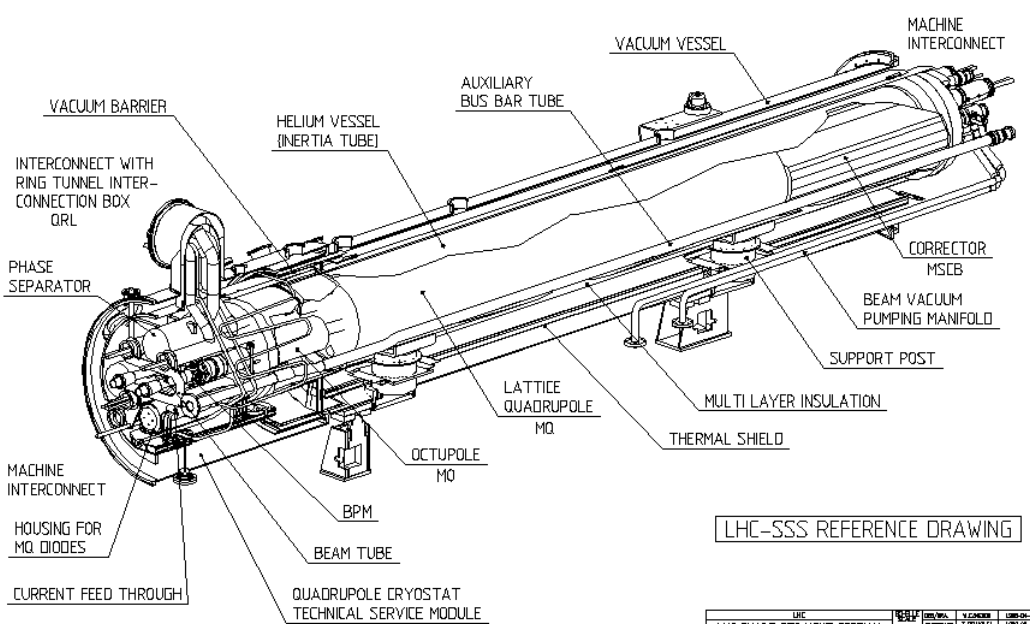
### 3.4 Dipole cryostat

The vacuum vessel consists of a long cylindrical standard tube with an outer diameter of 914 mm (36 inches) and a wall thickness 12 mm. It is made from alloyed low-carbon steel. The vessel has stainless steel end flanges for vacuumtight connection via elastomer seals to adjacent units. Three support regions feature circumferential reinforcement rings. Upper reinforcing angles support alignment fixtures. An ISO-standard flanged port is located azimuthally on the wall of the vessel at one end. In normal operation, the vessel will be under vacuum. In case of a cryogenic leak, the pressure can rise to 0.14 MPa absolute, and a sudden local cooling of the vessel wall to about 230 K may occur. The steel selected for the vacuum vessel wall is tested to demonstrate adequate energy absorption during a standard Charpy test at  $-50^{\circ}\text{C}$ . A front view of the cryodipole is shown in figure 3.5.

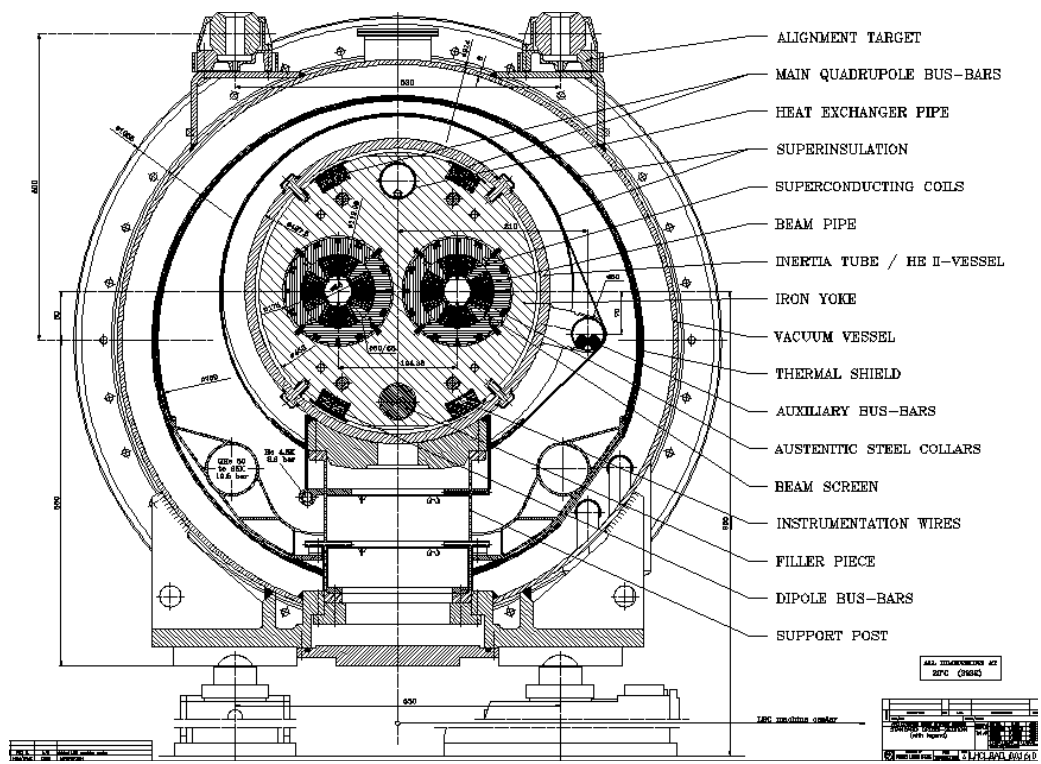
### 3.5 Short straight sections of the arcs

Figure 3.6 shows a perspective view while figure 3.7 illustrates the cross-section of an SSS. The cold masses of the arc SSSs contain the main quadrupole magnets, MQ, and various corrector magnets. On the upstream end, these can be either octupoles, MO, tuning quadrupoles, MQT, or skew quadrupole correctors, MQS. On the downstream end the combined sextupole-dipole correctors, MSCB are installed. These magnets are mounted inside a so-called inertia tube which is closed by end covers. This structure provides the helium vessel for these magnets and at the same time the mechanical stiffness of the assembly. The upstream flat end cover also supports the beam position monitors and the container for the quench protection diode stack of the main quadrupoles. The downstream, dished end cover has the connection tubes mounted with bellows for the interconnections to the adjacent dipole cold mass. Running through the SSSs are the two beam tubes, the heat exchanger tube, and the main dipole and quadrupole bus-bars as well as the spool bus-bars which interconnect the correctors of the dipole cold masses. The powering of the corrector magnets inside the short straight section cold masses is made via bus-bars placed in a tube located outside the cold mass, called line N. The cold masses are mounted into their cryostats to which the technical service modules, called QQS, are attached on the upstream end. These modules house the interconnections to the adjacent upstream dipole, the outlets of the wires for the instrumentation, and local corrector powering. In every second unit, the interconnection to the separate cryogenic feed line (QRL) and the phase separators are present. One out of four straight sections is equipped with a vacuum barrier for sectorising the cryostat vacuum. At the same positions, there are connection tubes and pressure plugs inside the upstream bus-bars to separate the local helium circuits of the machine.

Because of the lower electromagnetic forces, the two apertures do not need to be combined, but are assembled in separate annular collaring systems. This is in contrast to the case of the main dipoles. Computations, since confirmed by measurements, have shown that the magnetic coupling between the two apertures is negligible. This remains true even when the two apertures are excited with very different currents. Table 3.5 shows the design parameters of the main quadrupoles.



**Figure 3.6:** Short straight section with jumper.



**Figure 3.7:** Cross-section of SSS at quadrupole cold mass inside cryostat.

**Table 3.5:** Parameter list for main quadrupole magnets at 7.0 TeV.

Integrated Gradient	690	T
Nominal Temperature	1.9	K
Nominal Gradient	223	T/m
Peak Field in Conductor	6.85	T
Temperature Margin	2.19	K
Working Point on Load Line	80.3	%
Nominal Current	11870	A
Magnetic Length	3.10	m
Beam Separation distance (cold)	194.0	mm
Inner Coil Aperture Diameter (warm)	56.0	mm
Outer Coils Diameter	118.44	mm
Outer Yoke diameter	452	mm
Collar Material	Austenitic Steel	
Yoke Material	Low Carbon Steel	
Yoke Length including End Plates	3250	mm
Cold Mass Length Between End Covers	5345	mm
Total Mass Including Correctors	6500	kg
Number of turns per Coil (pole)	24	
Number of turns per coil inner layer (2 blocks)	2+8	
Number of turns per coil outer layer (2 blocks)	7+7	
Cable length per coil (pole)	160	m
Cable length per two-in-one quadrupole	1280	m
Bare Cable	Same as dipole outer layer	
Insulation Thickness 1 <sup>st</sup> layer	50	$\mu\text{m}$
2 <sup>nd</sup> layer	37.5	$\mu\text{m}$
3 <sup>rd</sup> layer (adhesive)	50+5	$\mu\text{m}$
Self-inductance, one aperture	5.6	mH
Stored energy, one aperture	395	KJ
Electromagnetic forces: Resultant in x-dir	537	KN
Resultant in y-dir	-732	KN

### 3.6 Orbit and multipole correctors in the arcs

About 3'800 single aperture and 1'000 twin aperture corrector magnets will be used in the LHC. The 194 mm beam separation gives sufficient lateral space to build all correctors as single bore modules, with a nominal working point between 40 – 60% along the load line. Twin aperture units

**Table 3.6:** Overview of corrector magnet types and location.

Name	Description	Location
MCS	Sextupole multipole corrector	Main MBA & MBB dipoles
MCDO	Nested Decapole-Octupole multipole corrector	Main MBA dipoles
MSCB	Sextupole-Dipole Corrector (lattice chromaticity & orbit). Exists in 4 variants with all combinations of normal & skew fields.	Main quadrupoles (SSS), dispersion suppressors
MQT, MQS	Tuning and Skew Quadrupoles	Main quadrupoles (SSS)
MO	Octupole Lattice Corrector (Landau damping)	Main quadrupoles (SSS)
MCBC, MCBY	Dipole correctors (orbit)	Insertion region and dispersion suppressors
MQTL	Long Trim Quadrupole	Insertion region and dispersion suppressors
MCBX MCBXA = MCBX+MCSTX	Inner Triplet nested Horizontal & Vertical Dipole Orbit corrector. MCBX with a nested 6-pole, 12-pole corrector insert.	Inner Triplets
MQSX	Skew quadrupole	Inner Triplets
MCSEX	Nested skew sextupole, octupole, skew octupole corrector package	Inner Triplets

are assembled by keying corresponding modules into laminated support structures. The assembly by keying ensures mechanical precision and allows flexibility during mounting, since the same type of module is used for a normal or skew magnet. To optimise the cost of the corrector magnets, common design and fabrication principles are applied. A summary of the corrector magnet types is given in table 3.6.

### 3.7 Insertion magnets

The insertion magnets are superconducting or normal conducting and are used in the eight insertion regions of the LHC. Four of these insertions are dedicated to experiments, while the others are used for major collider systems (one for the RF, two for beam cleaning, and one for beam dumping). The various functions of the insertions are fulfilled by a variety of magnets, most based on the technology of NbTi superconductors cooled by superfluid helium at 1.9 K. A number of stand-alone magnets in the matching sections and beam separation sections are cooled to 4.5 K, while in the radiation areas, specialised normal conducting magnets are installed. The different magnet types will be described in the following sections, organized according to the machine sectors to which they belong. The type and distribution of magnets amongst the eight insertions are summarized in table 3.7.

**Table 3.7:** Types and number of magnets used in the LHC insertion regions.

Magnet type	IR1 ATLAS	IR2 ALICE	IR3 Cleaning	IR4 RF	IR5 CMS	IR6 Dump	IR7 Cleaning	IR8 LHCb
<b>Main dipoles and quadrupoles (DS)</b>								
MB	16	16	16	16	16	16	16	16
MQ	2	2	10	2	2	2	10	2
<b>Superconducting insertion quadrupoles and correctors (DS and MS)</b>								
MQMC	2	2	-	2	2	2	-	2
MQM	6	10	-	4	6	2	-	10
MQML	8	6	-	4	8	4	-	6
MQY	2	6	-	4	2	4	-	6
MQTL	2	2	24	2	2	2	24	2
MSCB	2	2	2	2	2	2	2	2
MCBC	12	13	10	8	12	6	10	13
MCBY	6	9		4	6	4		9
<b>Normal conducting quadrupoles (Cleaning insertions)</b>								
MQWA/B(Q4,Q5)	-	-	24	-	-	-	24	-
<b>Superconducting separation dipoles</b>								
MBX (D1)	-	2	-	-	-	-	-	2
MBRC (D2)	2	2	-	-	2	-	-	2
MBRS (D3)	-	-	-	4	-	-	-	-
MBRB (D4)	-	-	-	4	-	-	-	-
<b>Normal conducting separation and correction dipoles</b>								
MBXW (D1)	12	-	-	-	12	-	-	-
MBW (D3)/(D4)	-	-	12	-	-	-	8	-
MCBWH/V	-	-	8	-	-	-	8	-
<b>Inner triplets and associated correctors</b>								
MQXA (Q1, Q3)	4	4	-	-	4	-	-	4
MQXB (Q2)	4	4	-	-	4	-	-	4
MCBX	6	6	-	-	6	-	-	6
MQSX	2	2	-	-	2	-	-	2
Multipole packages	2	2	-	-	2	-	-	2
<b>Normal conducting compensator dipoles in ALICE and LHCb experiments</b>								
MBWMD	-	1	-	-	-	-	-	-
MBXWT	-	2	-	-	-	-	-	-
MBXWH	-	-	-	-	-	-	-	1
MBXWS	-	-	-	-	-	-	-	2

### 3.8 Dispersion suppressors

The main dipoles in the dispersion suppressors have the same characteristics and the same cryostats as the arc, with a minor difference in the cryogenic circuits in some of the cryodipoles. These

**Table 3.8:** Main parameters of the dispersion suppressor quadrupole cold masses.

Cold mass position	Magnets	Operating temperature (K)	Length (mm)	Mass (kg)	No. units
Q11	MQ+MQTL+MSCB	1.9	6620	7416	16
Q10, Q8 (other than IR3/7)	MQML+MCBC	1.9	6620	7416	24
Q10, Q8 (IR3/7)	MQ+MQTL+MCBC	1.9	6620	7416	8
Q9 (other than IR3/7)	MQMC+MQM+MCBC	1.9	8020	9310	12
Q9 (IR3/7)	MQ+2 MQTL+MCBC	1.9	8020	9310	4

dipoles are installed two per half-cell. The half-cell from Q10 to Q11 is longer than the others, and the extra length is bridged by a connection cryostat, which is adjacent to quadrupole Q11 in all IRs. The connection cryostats ensure the continuity of the beam pipes, the cryogenic fluids, and the electrical bus-bars.

The superconducting quadrupoles in the dispersion suppressors are based on the MQ and MQM-type magnets (next section). The main parameters of the dispersion suppressor quadrupole cold masses are given in table 3.8. Their cryostats closely follow the design of the SSS cryostat, where the standard section of the vacuum vessel is modified in accordance with the length of the cold mas.

### 3.9 Matching section quadrupoles

The tuning of the LHC insertions is provided by the individually powered quadrupoles in the matching and dispersion suppressor sections. The matching sections consist of stand-alone quadrupoles arranged in four half cells, but the number and parameters of the magnets are specific for each insertion. Apart from the cleaning insertions, where specialized normal conducting quadrupoles are used in the high-radiation areas, all matching quadrupoles are superconducting magnets. Most of them are cooled to 4.5 K, except the Q7 quadrupoles, which are the first magnets in the continuous arc cryostat and are cooled to 1.9 K.

CERN has developed two superconducting quadrupoles for the matching sections: the MQM quadrupole, featuring a 56 mm aperture coil, which is also used in the dispersion suppressors, and the MQY quadrupole, with an enlarged, 70 mm coil aperture. Both quadrupoles use narrow cables, so that the nominal current is less than 6 kA, substantially simplifying the warm and cold powering circuits. Each aperture is powered separately, but a common return is used, so that a three-wire bus-bar system is sufficient for full control of the apertures.

The MQM quadrupole, figure 3.8, consists of two identical, independently powered apertures, which are assembled together in a two-in-one yoke structure. Three versions of the MQM quadrupole are required for the LHC, with magnetic lengths of 2.4 m, 3.4 m and 4.8 m. The main parameters of the quadrupole are listed in table 3.9. In total, 84 MQM magnets are required for the LHC dispersion suppressors and matching sections.

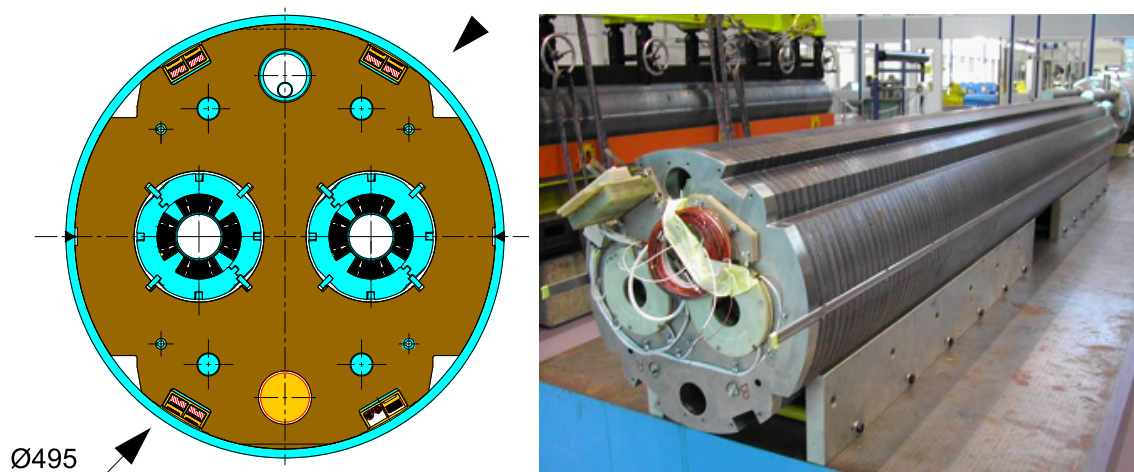


**Figure 3.8:** Cross-section of MQM quadrupole (left) and a 5 m long MQM magnet on the test stand (right) (dimensions in mm).

**Table 3.9:** Main parameters of the MQM-type quadrupoles.

Coil inner diameter	56 mm
Magnetic length	2.4/3.4/4.8 m
Operating temperature	1.9/4.5 K
Nominal gradient	200/160 T/m
Nominal current	5390/4310 A
Cold bore diameter OD/ID	53/50 mm
Peak field in coil	6.3 T
Quench field	7.8 T
Stored energy per aperture	64.3 kJ/m
Inductance per aperture	4.44 mH
Quench protection	Quench heaters, two independent circuits
Cable width	8.8 mm
Mid-thickness	0.84 mm
Keystone angle	0.91 deg.
No of strands	36
Strand diameter	0.475 mm
Cu/SC Ratio	1.75
Filament diameter	6 $\mu$ m
$j_c$ , (4.2 K and 5 T)	2800 A/mm <sup>2</sup>
Mass (2.4/3.4/4.8 m)	3100/4300/6000 kg

The MQY wide-aperture quadrupole, figure 3.9, consists of two individually powered apertures assembled in a common yoke structure. The coil aperture of the magnet is 70 mm and its magnetic length 3.4 m. The main parameters of the quadrupole are given in table 3.10. In total, 24 MQY magnets are required for the LHC matching sections.

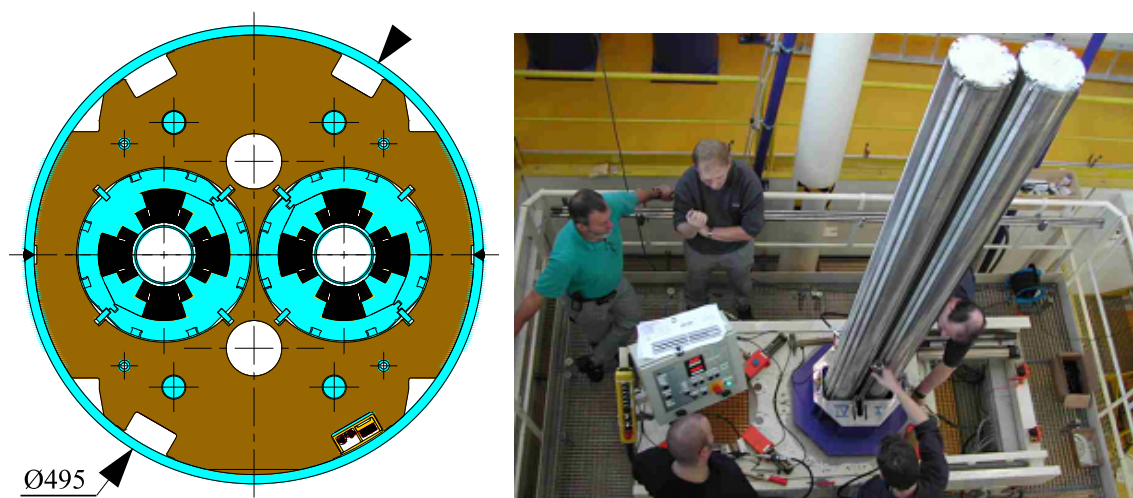


**Figure 3.9:** Cross-section of MQY quadrupole (left) and assembly of the magnet (right) (dimensions in mm).

**Table 3.10:** Main parameters of the MQY matching quadrupole.

Coil inner diameter	70 mm
Magnetic length	3.4 m
Operating temperature	4.5 K
Nominal gradient	160 T/m
Nominal current	3610 A
Cold bore diameter OD/ID	66.5/62.9 mm
Peak field in coil	6.1 T
Quench field	7.5 T
Stored energy	479 kJ
Inductance	73.8 mH
Quench protection	Quench heaters, two independent circuits
Cable width, cable 1/2	8.3/8.3 mm
Mid-thickness, cable 1/2	1.285/0.845 mm
Keystone angle, cable 1/2	2.16/1.05 deg.
No of strands, cable 1/2	22/34
Strand diameter, cable 1/2	0.735/0.475 mm
Cu/SC Ratio, cable 1/2	1.25/1.75
Filament diameter, cable 1/2	6/6 $\mu\text{m}$
$j_c$ , cable 1/2, (4.2 K and 5 T)	2670/2800 A/mm <sup>2</sup>
Mass	4400 kg

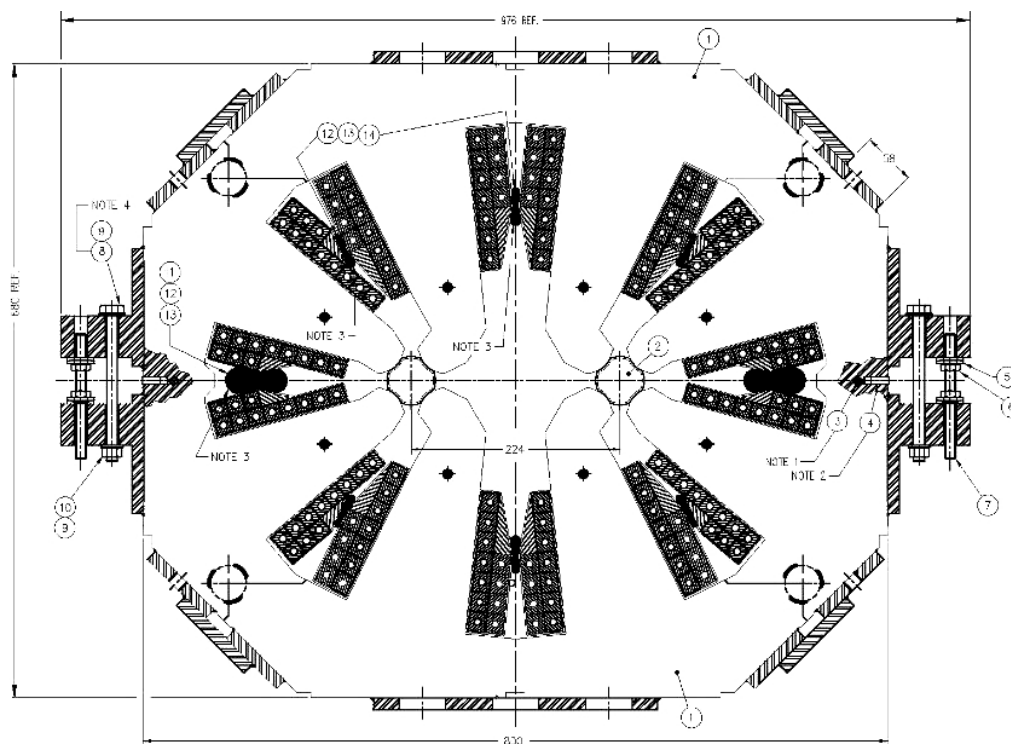


**Figure 3.10:** Cross-section of the MQW twin aperture normal conducting matching quadrupole (dimensions in mm).

In the cleaning insertions IR3 and IR7, each of the matching quadrupoles Q4 and Q5 consists of a group of six normal conducting MQW magnets. This choice is dictated by the high radiation levels due to scattered particles from the collimation system, and therefore the use of superconducting magnets is not possible. The cross-section of the quadrupole is shown in figure 3.10. It features two apertures in a common yoke (2-in-1), which is atypical for normal conducting quadrupole magnets, but is needed because of transverse space constraints in the tunnel. The two apertures may be powered in series in a standard focusing/defocusing configuration (MQWA), or alternatively in a focusing/focusing configuration (MQWB) in order to correct asymmetries of the magnet. In a functional group of six magnets, five are configured as MQWA, corrected by one configured as MQWB. As in most normal conducting magnets, the field quality is iron-dominated and therefore defined by the shape of the magnetic poles. In order to achieve the necessary field quality, the separation between poles is adjusted and verified to within a tenth of a millimetre by tightening rods along the length of the magnet. The total number of quadrupole magnets in each of the two insertions is 24. Altogether 52 magnets of this type, including 4 spares, have been built by Canadian industry in collaboration with TRIUMF and CERN. The design parameters are given in table 3.11.

### 3.10 Matching section separation dipoles

The separation dipoles are used in several insertions to change the beam separation from the nominal 194 mm in the LHC arcs. In the experimental insertions, a pair of D1-D2 dipoles brings the two beams onto a collision orbit at the IP and then separates the beams again beyond the IP. To reduce

**Table 3.11:** Main parameters of the MQW normal conducting quadrupole magnet.

Magnet type	MQWA	MQWB
Magnetic length	3.1 m	
Beam separation	224 mm	
Aperture diameter	46 mm	
Operating temperature	< 65° C	
Nominal gradient	35 T/m	30 T/m
Nominal current	710 A	600 A
Inductance	28 mH	
Resistance	37 mΩ	
Conductor X-section	20.5 x 18.0 mm <sup>2</sup> inner poles 17.0 x 17.0 mm <sup>2</sup> outer poles	
Cooling hole diameter	7 mm inner poles, 8 mm outer poles	
Number of turns per magnet	8 x 11	
Minimum water flow	28 l/min	
Dissipated power at I <sub>nom</sub>	19 kW	14 kW
Mass	11700 kg	

the long-range beam-beam effects, the first separation dipole D1 is placed immediately upstream of the low- $\beta$  triplet. In the high-luminosity insertions, high radiation levels are expected, and more robust normal conducting magnets, MBXW, are used. In the ALICE and LHCb insertions, D1 is a stronger superconducting magnet, MBX, allowing more space for the injection systems. In all cases, the D2 separation dipole, MBRC, is a twin-aperture superconducting magnet. In the cleaning insertions, the pair of D3-D4 dipoles separates the beams to 224 mm to accommodate the collimation system, while in the RF insertion the beam separation is 420 mm, so that individual RF cavities can be installed for each beam. The radiation levels in the cleaning insertions require the use of normal conducting dipoles, MBW (both for D3 and D4), while superconducting dipoles, MBRB (D4) and MBRS (D3), are used in the RF insertion.

The MBX (D1), MBRB/C (D4/D2) and MBRS (D3) dipoles are designed and built by BNL (USA) on the basis of the RHIC lattice dipole [21]. The MBX magnets are designed with one RHIC-style cold mass in a RHIC-style cryostat, and the MBRS magnets are designed with two such cold masses side-by-side in a common cryostat. The cold masses are built straight, without the 47 mm sagitta of the RHIC magnets. The MBRB and MBRC magnets are built with coils that are pre-stressed with stainless steel collars. These collared coils are assembled into yokes with common outside dimensions but with two aperture spacing, depending on the type. The main parameters of the magnets are given in table 3.12.

The MBX dipole cross-section is shown in figure 3.11. Many of its design features are identical to the RHIC main dipoles. However, the magnet is equipped with two heat exchangers, allowing it to be cooled to 1.9 K, and it has a larger cold bore (OD 78 mm) than the RHIC dipole. Another feature is the use of quench heaters as active protection elements. These modifications require additional cryogenic and electrical instrumentation compared to the original RHIC design.

**Table 3.12:** Main parameters of the MBX, MBRB/C and MBRS superconducting separation dipoles.

Coil inner diameter	80 mm
Magnetic length	9.45 m
Nominal field	3.8 T
Operating temperature	1.9 K (MBX) 4.5 K (MBRB/C, MBRS)
Nominal current	5750 A (MBX, MBRS) 6050 A (MBRB/C)
Aperture separation	188 mm (MBRC) 194 mm (MBRB) 414 mm (MBRS)
Cold bore diameter OD/ID	78/74 mm (MBX) 73/69 mm (MBRB/C, MBRS)
Peak field in coil	4.2 T
Quench field	4.8 T
Stored energy per aperture	470 kJ
Inductance per aperture	25.8 mH
Quench protection	Quench heaters, two independent circuits per aperture
Cable width	9.73 mm
Mid-thickness	1.166 mm
Keystone angle	1.2 deg.
No of strands	30
Strand diameter	0.648 mm
Cu/SC Ratio	1.8
Filament diameter	6 $\mu$ m
$j_c$	2500 A/mm <sup>2</sup> (4.2 K and 5 T)
Mass	4500 kg (MBX) 13500 kg (MBRS) 24500 kg (MBRB/C)

The MBRB magnet is a two-in-one magnet with parallel fields in the two apertures. The MBRC is similar in design (its cross-section is shown in figure 3.12) and differs only by the nominal aperture spacing (188 mm). In addition, to allow installation of the beam screens, the cold bore in MBRB is slightly off-centred from the IP side. The cross-talk between parallel fields in the two apertures is reduced by additional iron around the median plane, resulting in an oval shape of the cold mass. Its outer dimensions are identical in the vertical plane to the LHC main dipole, so that standard LHC support posts and other cryostat elements can be used in a 9.8 m long vacuum tank.

The MBRS separation dipole consists of two MBX-like cold masses assembled in a 9.6 m long cryostat, as shown in figure 3.13. The cold masses are aligned to a separation of 414 mm

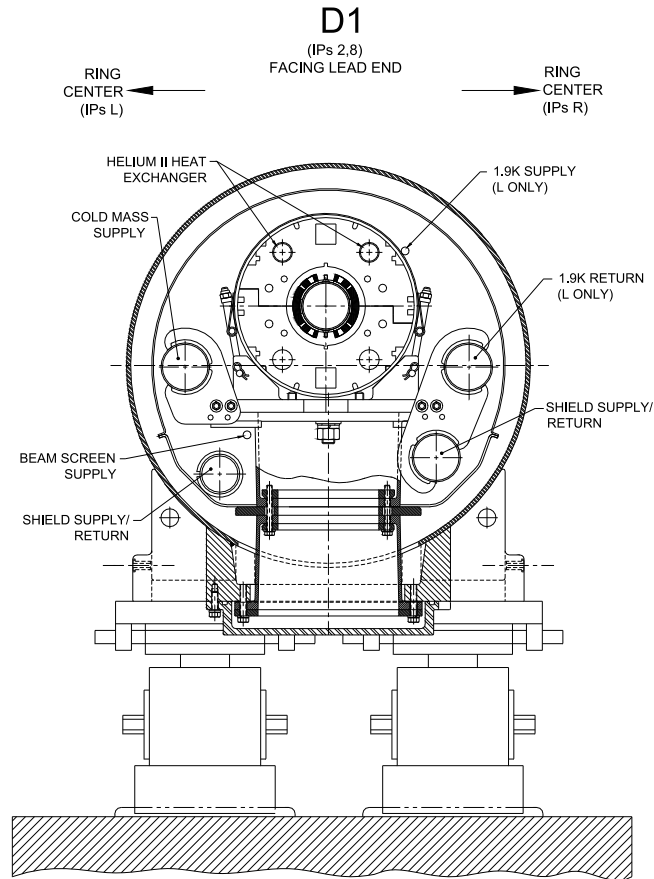


**Figure 3.11:** Cross-section of the MBX (D1) cryodipole, of same design as the RHIC main dipole.

using three transverse beams, connected to the upper plates of standard LHC dipole posts. Other cryostat elements are identical to MBRB. The magnet interfaces on the non-IP side with the QQS service module, which provides the connection to the cryogenics and powering services. On the IP side, provisions are made for interconnecting MBRS with the MSRU undulator [22] designed to produce synchrotron radiation for transversal beam profile measurement.

The MBW and MBXW normal conducting dipoles are designed and built by BINP, Novosibirsk, Russia, employing a well-established technology of epoxy-impregnated coils in a laminated window-frame steel yoke: see figures 3.14 and 3.15. The two coils of both types of magnet consist of three pancakes that are wound from a hollow rectangular copper conductor. The conductor is insulated with glass-fibre tape and impregnated with epoxy resin. The yoke is laminated from insulated magnetic steel sheets of 1.5 mm thickness to reduce eddy currents that are generated during ramping. The laminations are held together by welded plates. The shape of the end-plates and shims is adjusted to compensate the magnetic end effects. The coils are fixed in the yoke by stainless steel clamps at the end of the magnet and further supported by separation blocks in the mid-plane. The magnets are manufactured as two half-cores that are clamped together with studs and nuts along the side cover plates. The main parameters of the magnets are given in table 3.13.

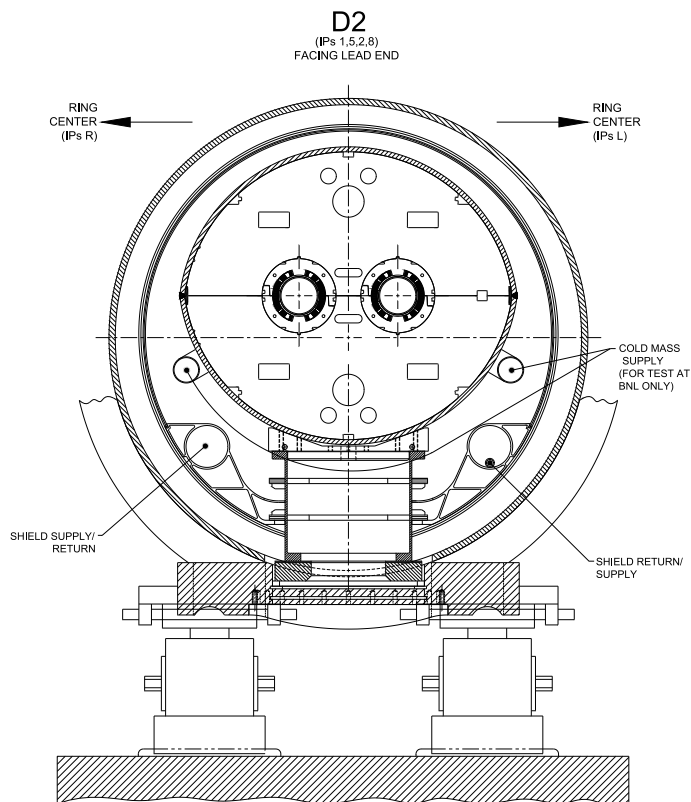


**Figure 3.12:** Cross section of the MBRC (D2) cryodipole at a support post location.

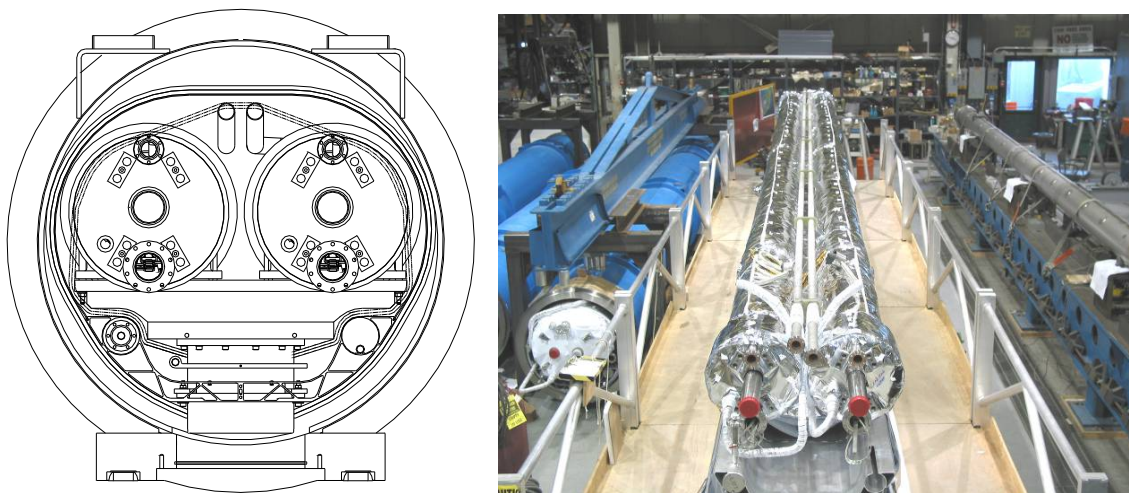


**Figure 3.13:** Cross-section of the MBRS dipole (left) and assembly of the MBRS cold masses at BNL (right).

The field quality of normal conducting magnets is defined by the shape of the steel poles. In order to guarantee good field quality, the punching of the laminations is controlled to within 0.05 mm in the vicinity of the apertures. The lamination stacks and the clamping of the two half-magnets

**Table 3.13:** Main parameters of the MBW and MBXW separation dipoles.

Magnet type	MBW	MBXW
Magnetic length	3.4 m	
Beam separation	194–224 mm	0–27 mm
Gap height	52 mm	63 mm
Coil Protection temperature	< 65° C	
Nominal field	1.42 T	1.28 T
Nominal current	720 A	690 A
Inductance	180mH	145 mH
Resistance	55 mΩ	60 mΩ
Conductor X-section	18 x 15 mm <sup>2</sup>	
Cooling hole diameter	8 mm	
Number of turns per magnet	2 x 42	2 x 48
Minimum water flow	19 l/min	
Dissipated power at $I_{nom}$	29kW	29 kW
Mass	18000 kg	11500 kg

are also controlled to within a tenth of a millimetre. Access to the laminations on the top and the sides of the magnet allows the verification of the magnet assembly after production. Specifications require a sag of less than 0.5 mm and a twist of less than 1 mrad. All these parameters are checked to assure quality during production and to guarantee the required field quality.

The MBW magnet, shown in figure 3.14, features a pole shape with varying gap height and two positions for the beam pipes (194 mm to 224 mm), while employing a standard H-type dipole construction. The two coils consist of three pancakes with 14 windings. The overall number of MBW magnets produced by BINP is 24, including 4 spares.

The cross-section of the MBXW, shown in figure 3.15, features a coil with three pancakes with 16 turns each, wound using the same copper conductor as for the MBW. Since both beams run through a single pipe, the pole region is 120 mm wide with a gap height of 63 mm. Small shims, placed along the sides of the pole, are part of the punched laminations and homogenize the field in the aperture. The total number of MBXW magnets built by BINP is 29, including 4 spares.

### 3.11 Low-beta triplets

The low- $\beta$  triplet, figure 3.16, is composed of four single-aperture quadrupoles with a coil aperture of 70 mm. These magnets are cooled with superfluid helium at 1.9 K using an external heat exchanger system capable of extracting up to 10 W/m of power deposited in the coils by the secondary particles emanating from the proton collisions. Two types of quadrupoles are used in the triplet: 6.6 m long MQXA magnets designed and developed by KEK, Japan, and 5.7 m long MQXB magnets designed and built by FNAL, USA. The magnets are powered in series with 7 kA, with an additional inner loop of 5 kA for the MQXB magnets. Together with the orbit correctors MCBX, skew quadrupoles MQSX, and multipole spool pieces supplied by CERN, the low- $\beta$  quadrupoles

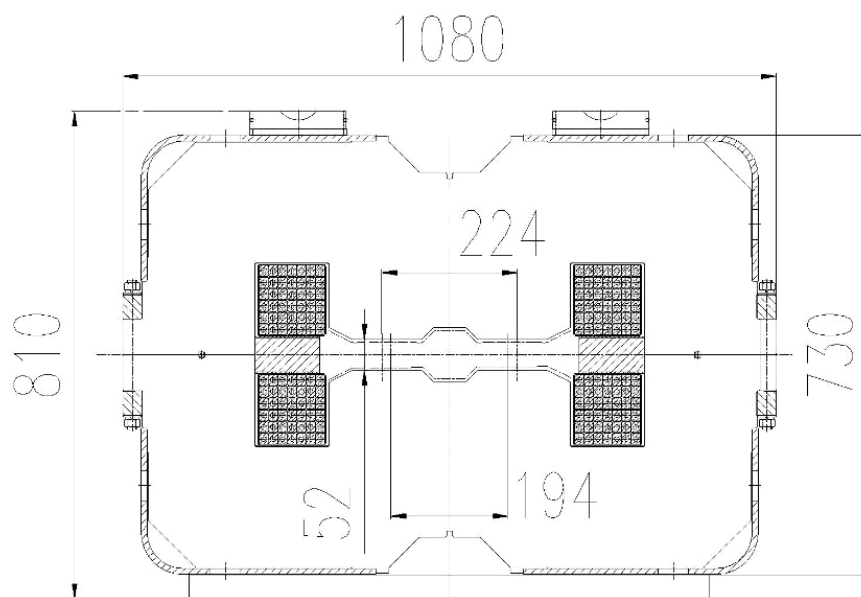


**Figure 3.14:** Cross-section of the normal conducting separation dipole MBW (dimensions in mm).

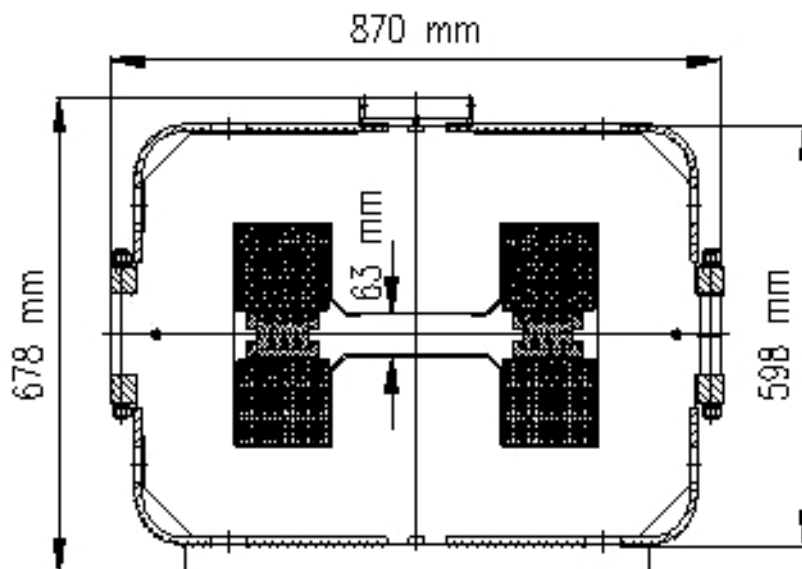


**Figure 3.15:** Cross-section of the normal conducting separator dipole magnet MBXW.

are completed in their cold masses and cryostated by FNAL. The cryogenic feed-boxes (DFBX), providing a link to the cryogenic distribution line and power converters, are designed and built by LBNL, USA.

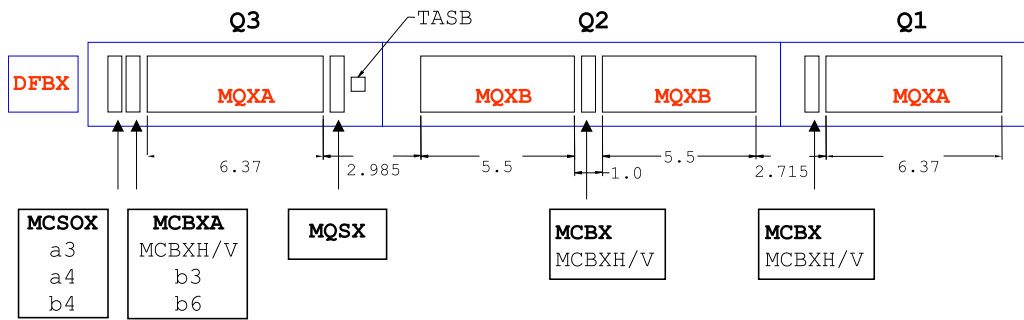


**Figure 3.16:** Schematic layout of the low- $\beta$  triplet (distances in m).

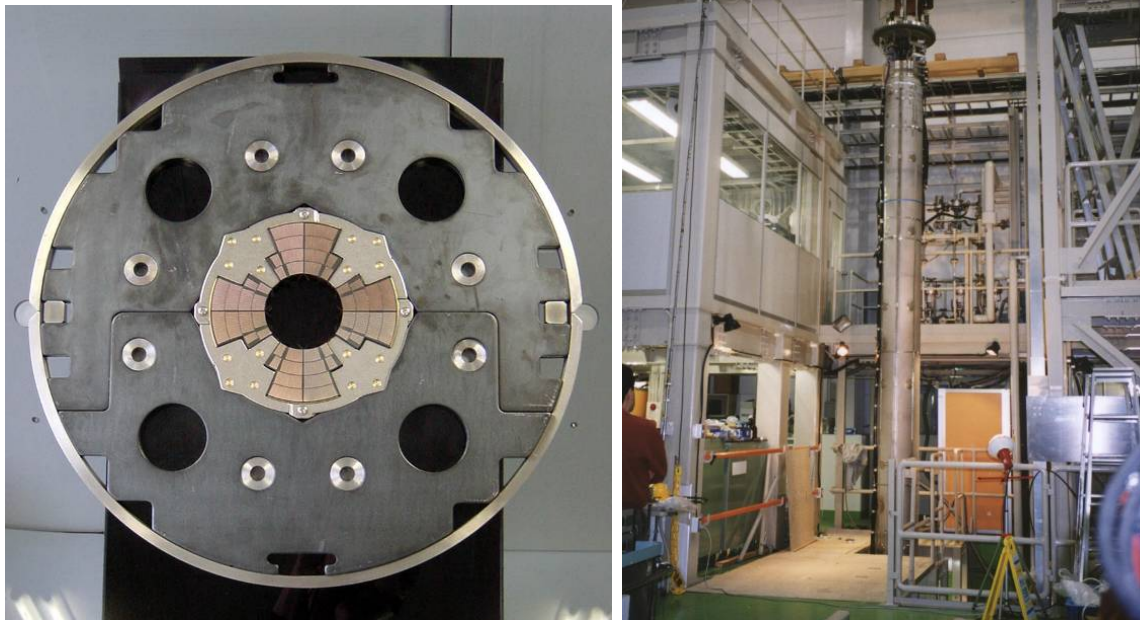


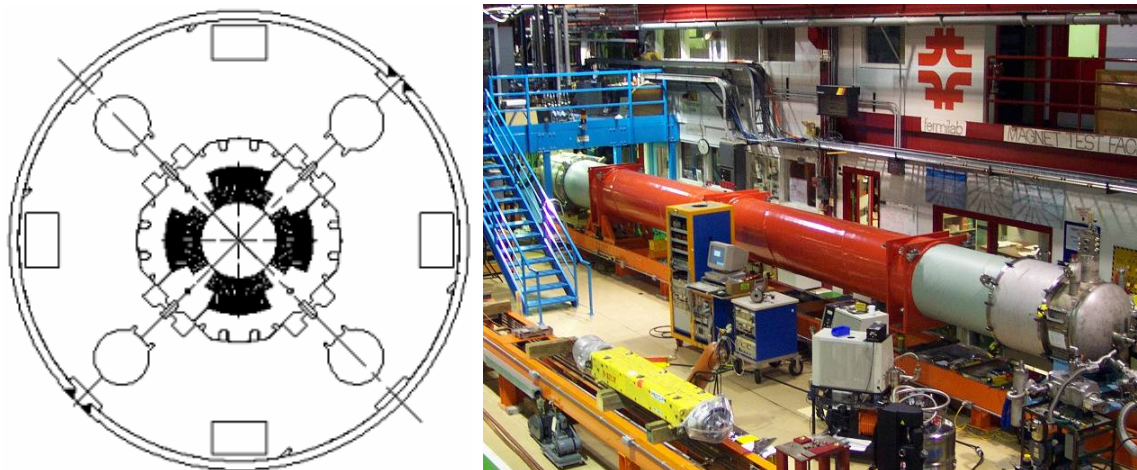
**Figure 3.17:** Cross-section of the MQXA low- $\beta$  quadrupole (left) and MQXA quadrupole ready for tests in the vertical cryostat at KEK (right).

Alongside the LHC main dipoles, the high-gradient, wide-aperture low- $\beta$  quadrupoles are the most demanding magnets in the collider. They must operate reliably at 215 T/m, sustain extremely high heat loads in the coils and high radiation dose during their lifetime, and have a very good field quality within the 63 mm aperture of the cold bore.

The design of the MQXA quadrupole is based on a four-layer coil using 11 mm wide Rutherford-type graded NbTi cables. The coils are wound and cured in two double layers and are assembled using 10 mm wide spacer-type collars (see figure 3.17). The pre-stress in the coils and their rigidity is provided by the yoke structure, which consists of horizontally split laminations keyed at the mid-plane. The main parameters of the magnet are given in table 3.14.

**Table 3.14:** Main parameters of the MQXA low- $\beta$  quadrupole.

Coil inner diameter	70 mm
Magnetic length	6.37 m
Operating temperature	1.9 K
Nominal gradient	215 T/m
Nominal current	7149 A
Cold bore diameter OD/ID	66.5/62.9 mm
Peak field in coil	8.6 T
Quench field	10.7 T
Stored energy	2300 kJ
Inductance	90.1 mH
Quench protection	Quench heaters, two independent circuits
Cable width, cable 1/2	11/11 mm
Mid-thickness, cable 1/2	1.487/1.340 mm
Keystone angle, cable 1/2	2.309/1.319 deg.
No of strands, cable 1/2	27/30
Strand diameter, cable 1/2	0.815/0.735 mm
Cu/SC Ratio, cable 1/2	1.2/1.9
Filament diameter, cable 1/2	10/10 $\mu\text{m}$
$j_c$ , cable 1/2, (4.2 K and 6 T)	2200/2160 A/mm <sup>2</sup>
Mass	9600 kg

**Figure 3.18:** Cross-section of the MQXB low- $\beta$  quadrupole (left) and Q2 quadrupole on test in FNAL (right).

The MQXB design features a two-layer coil, with each layer individually wound using a 15.4 mm wide Rutherford-type NbTi cable (see figure 3.18). The coils are assembled using free-standing collars, which provide the pre-stress and counteract the magnetic forces. The collared

**Table 3.15:** Main parameters of the MQXB low- $\beta$  quadrupole.

Coil inner diameter	70 mm
Magnetic length	5.5 m
Operating temperature	1.9 K
Nominal gradient	215 T/m
Nominal current	11950 A
Cold bore diameter OD/ID	66.5/62.9 mm
Peak field in coil	7.7 T
Quench field	9.2 T
Stored energy	1360 kJ
Inductance	19.1 mH
Quench protection	Quench heaters, two independent circuits
Cable width, cable 1/2	15.4/15.4 mm
Mid-thickness, cable 1/2	1.456/1.146 mm
Keystone angle, cable 1/2	1.079/0.707 deg.
No of strands, cable 1/2	37/46
Strand diameter, cable 1/2	0.808/0.650 mm
Cu/SC Ratio, cable 1/2	1.3/1.8
Filament diameter, cable 1/2	6/6 $\mu\text{m}$
$j_c$ , cable 1/2 (4.2 K and 5 T)	2750/2750 A/mm <sup>2</sup>
Mass	5700 kg

assembly is aligned in the yoke structure with precision keys, and the magnet is enclosed in a stainless steel helium vessel consisting of half-shells welded at the pole plane. The design parameters of the magnet are given in table 3.15.

There are also a number of superconducting and normal conducting corrector magnets in the insertions.

### 3.12 Compensator dipoles in ALICE and LHCb experiments

The effect of the spectrometer dipoles in the ALICE (IR2) and LHCb (IR8) experiments on the beam is compensated in both cases with three dipoles, one placed symmetrically with respect to the IP and two weaker dipoles placed next to the inner triplets. The dipole field of the ALICE spectrometer, which produces a vertical kick on the beam, is compensated with a MBWMD and two MBXWT magnets. The MBWMD is a magnet from the SPS complex, originally built for the ISR beam lines (type HB2, turned vertical). Its main parameters are shown in table 3.16, and its cross section is shown in figure 3.19. The LHCb dipole, which produces a horizontal kick on the beam, is compensated by an MBXWH magnet and two MBXWS magnets. The MBXWH is in fact an MBXW separation dipole, discussed above, and the MBXWT and MBXWS magnets are short versions of the MBXW dipole. The parameters of these magnets are given in table 3.16. All MBXW type magnets are designed and built by BINP, Russia.

**Table 3.16:** Main parameters of the compensator dipoles for ALICE and LHCb (the magnets in the first three columns have the same cross-section as MBXW).

Magnet type	MBXWH	MBXWT	MBXWS	MBWMD
Magnetic length	3.4 m	1.5 m	0.8 m	2.6 m
Gap height		63 mm		80 mm
Coil protection temperature		< 65° C		< 65° C
Nominal field	1.24 T	1.20 T	1.33 T	1.32 T
Current at nominal field	670 A	630 A	780 A	475 A
Inductance	145 mH	70 mH	35 mH	639 mH
Resistance	60 mΩ	40 mΩ	20 mΩ	172 mΩ
Conductor X-section		18 x 15 mm <sup>2</sup>		16.3 x 10.8 mm <sup>2</sup>
Cooling hole diameter		8 mm		6.6 mm
Number of turns per magnet		2 x 48		2 x 102
Minimum water flow	19 l/min	5 l/min	7 l/min	20 l/min
Dissipated power at I <sub>nom</sub>	27 kW	16 kW	12 kW	39 kW
Mass	11500 kg	5800 kg	3700 kg	20500 kg

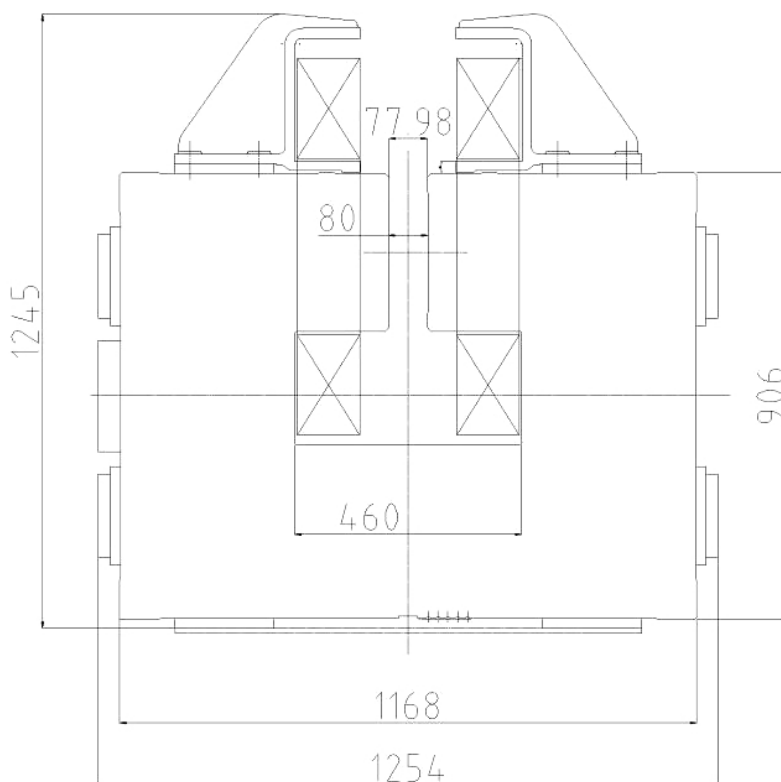


**Figure 3.19:** Cross-section of the normal conducting compensation dipole MBWMD for ALICE (dimensions in mm).